ARTICLE IN PRESS

Materials Today: Proceedings xxx (xxxx) xxx

Contents lists available at ScienceDirect

Materials Today: Proceedings

journal homepage: www.elsevier.com/locate/matpr

Memristive and biological synaptic behavior in transition metal dichalcogenide-WS_2 nanostructures: A review

Amarjit Khuraijam [a], Vipin Kumar [a,b,*], Nilanjan Halder [a], Anoop Kumar Mukhopadhyay [a,c]

[a] Department of Physics, School of Basic Science, Faculty of Science, Manipal University Jaipur, Jaipur 303007, Rajasthan, India
[b] Multiscale Research Simulation Center, Manipal University Jaipur, Jaipur 303007, Rajasthan, India
[c] Biyani Girls College, Vidyadhar Nagar, Jaipur-302039, Rajasthan, India

ARTICLE INFO

Article history:
Available online xxxx

Keywords:
Transition metal dichalcogenides
2D materials
WS_2 nanosheet
Memristors
Biological synapse

ABSTRACT

Recently, two dimensional (2D) layered materials are being identified as potential candidates for different device applications such as memristors and brain inspired computing. These materials exhibit unusual physical properties such as atomic thickness, mechanically robust, tunable electrical and optical properties. These fascinating properties of 2D materials are very difficult to achieve with traditional materials used for different electronic purposes. The 2D materials are promising for high performance synapses and artificial neurons because of their high energy efficiency, excellent scalability, and high integration density. The present article gives an overview on the properties of 2D transition metal dichalcogenides (WS_2) based electronic devices for memristive switching and biological synaptic behavior. Moreover, its integration into large-scale devices and associated challenges are being summarized along with the future prospective.

Selection and peer-review under responsibility of the scientific committee of the International Conference on Recent Advances in Modeling and Simulations Techniques in Engineering and Science.

1. Introduction

Memristor is a fourth fundamental circuit element. It is a non-volatile electronic memory device i.e. memristor based devices remember their state even after switching off their power. The first theoretical description of memristor was given by L. Chua in 1971 [1]. It is an amalgamation of "memory and resistor". It is a passive two terminal electrical component, which relates the time integral of current (electric charge) and magnetic flux through it. The resistance of a memristor is a function of charge flowed through it (alternatively, function of current). The resistance increases when current flows in one direction. However, the resistance of a memristor decreases when the current flows in the opposite direction, but never goes below zero. It signifies that the resistance of a memristor holds the value that it had earlier when the current is stopped. Alternatively, memristors "remember" the final value of current flowed through it. Hence, a memristor act as a memory as well as resistor.

In the electrical realm of science and technology, there were only three fundamental electrical components known namely: resistor (R), inductor (L) and capacitor (C). The fourth fundamental electrical component came into existence in 1971 [1], which is known as the memristor (M). There exist different types of memristor. The common characteristics of all type of memristor is that they possess a pinched hysteresis curve between current and voltage [2]. The shape of pinched hysteresis may vary because it depends on the device. However, it always passes through the origin. In 1976, Chua et al. generalized the concepts of memristors and memristive systems to demonstrate a physical device [3]. However, this work becomes more attractive for scientific community in 2008 when a physical model of memristor was presented by Williams and his collaborators [4,5]. The theory of memristors were explained on the TiO_2 based resistive switching by Hewlett Packard [4,5]. However, the resistance switching behavior in TiO_2 was reported in 1968 [6]. Initially, it was claimed that the TiO_2 based device is similar to an ideal memristor. The analytical expression for the proposed memristor structure is given by

$$M(X,I) = R_{on}\frac{X(t)}{D} + R_{off}\left(1 - \frac{X(t)}{D}\right); f(X,I) = \mu_v \frac{R_{on}}{D} I(t)$$

* Corresponding author.
E-mail address: vipin.kumar@jaipur.manipal.edu (V. Kumar).

https://doi.org/10.1016/j.matpr.2022.03.179
2214-7853/
Selection and peer-review under responsibility of the scientific committee of the International Conference on Recent Advances in Modeling and Simulations Techniques in Engineering and Science.

where, R_{on} and R_{off} are the resistances of the device when $X(t) = D$ and $X(t) = 0$. $X(t)$ is a stable variable and can vary with the dimension of the device (from zero to D, in the present case).

The memristor based physical device was demonstrated by scientists at HP lab in 2008. The behavior of this physical memristor was in good agreement with that of the Chua's memristor model presented in 1971 [1–5]. After this physical model of memristor, there were several models of memristor presented such as linear and nonlinear ionic drift model, Simmon model for different device applications and others [7–14]. The Strukov model (linear ionic drift model) was demonstrated by William and his collaborators. There was a serious problem with this model that it produces very high electric field upon changing the applied voltage by a small amount in nanoscale devices. It leads to the significant nonlinearities involved in the ionic transport in the linear ionic drift model. These nonlinearities can be controlled by the nonlinear type window function. This is incorporated in the nonlinear ionic drift model. There are different types of model presented based on the nonlinear type window function [15]. Biolek model is useful for logic circuits such as binary and ternary logic circuits. However, the fabrication process of Biolek model is more complex [16]. Moreover, its properties such as switching time, saturation frequency and I-V characteristics need to be more explored for further improvement of the device performance [17].

The nanoscale memristor is the most widely used in crossbar arrays to implement the cross-point devices [18,19]. The nanoscale-based devices have more advantages than conventional electronic devices such as high integration density [20,21], fast, power efficient and non-volatile [22,23]. These devices are useful in the different fields of electronics such as logic circuits [24], phase shift oscillators [25,26] and synaptic computing [27,28]. The memristors have been used to implement different hardware synapse. These synapses have been integrated for different applications [29].

After the successful demonstration of TiO_2 based memristor, the scientists have made good efforts to explore the physics of memristors with different materials such as polymer based memristors for memory and neuromorphic computing [30–34]. Bessonov et al. demonstrated a layered memristive and memcapacitive switching behavior of MoO_x/MoS_2 [35]. The memristive behavior has also been demonstrated in atomically thin nanosheets or nanomaterials such as MoS_2 [36–40]. The oxide based memristor devices requires large amount of power to operate. It opens an avenue to search the new materials for memristor based device applications that consume low power (i.e. energy efficient materials). Therefore, in the present brief review, the focus is made to discuss the WS_2 based devices for energy efficient electronic applications such as memristive and biological synaptic applications. This brief review is organized in the following manner: in the introduction part, a brief historical and the development of memristor is presented. In the second section, a brief theoretical description of memristor is discussed. In the third section, the overview on the WS2 based memristors and their properties are being discussed for different applications. Finally, the conclusion of the present work, challenges to successfully implement these devices to large scale devices along with future perspectives are discussed.

2. Theoretical description of memristor

Among four fundamental circuit variables q, I, V and ϕ, only five relationships among these fundamental circuit variables were known initially. These are as follows:

$$i = \frac{dq}{dt}, \quad R = \frac{dV}{di}, \quad C = \frac{dq}{dV}, \quad L = \frac{d\phi}{di}, \quad V = \frac{d\phi}{dt}$$

However, the sixth relationship between ϕ and q were not known. It was the missing relationship between these fundamental circuit variables. This missing relationship between q and ϕ were observed by Chua in 1971. It led to the existence of fourth fundamental electrical components known as memristor (M), which relates q and ϕ through the relation, $M = d\phi/dq$. Chua identified a symmetry between three nonlinear fundamental electrical components (R, L and C). Based on this symmetry, Chua deduced a fourth nonlinear fundamental electrical component that relates charge (q) and flux (ϕ). There is different type of memristors namely- current controlled or charge controlled memristors and voltage or flux-controlled memristors. A memristor can be characterized by a relation of the form, $f(\phi, q) = 0$. If $f(\phi, q) = 0$ is expressible as single valued function of charge, then this memristor is known as the charge controlled or current controlled memristor. On the other hand, if $f(\phi, q) = 0$ can be represented as a single valued function of flux, then it is called the voltage controlled or flux controlled memristor [1]. The voltage across a current controlled memristor is given by $V(t) = M(q(t))\, i(t)$, where, $M(q) = d\phi(q)/dq$. The memristance of memristor $M(q(t))$ has the unit of resistance. Similarly, the current of a flux controlled memristor can be written as follows: $i(t) = w(\phi(t))\, v(t)$, where, $w(\phi(t)) = dq(\phi)/d\phi$. The unit of $w(\phi(t))$ is that of conductance.

3. Transition metal dichalcogenide-WS_2 for memristive and synaptic applications

After successful demonstration of MoS_2 based memristors, researchers have taken equal interest in predicting the memristor characteristics in other TMD materials. Therefore, in the present article, we focus on the properties of WS_2 for memristor based electronic device applications and neuromorphic computing. Two dimensional memristive devices exhibits unique properties, hence, could be the potential candidate in neuromorphic computing [41–44]. The non-volatile switching behavior is also exhibited by sub-nanometer sized devices [45]. The quantum confinement in two dimensional materials leads to the unexpected physical and chemical properties. In the family of 2D materials, TMDs, with chemical formula MX_2 (M = metal and X = chalcogen), exhibit semiconducting properties [46]. Among 2D TMDs, MoS_2 and WS_2 have gained a great research interest in the scientific community for high performance memristive devices [43,44]. The properties of MoS_2 have been studied most widely for different electronic and photonic applications. MoS_2 has high on/off ratio of the order of 10^8 and band gap of 1.8 eV [47]. The on/off ratio of WS_2 is of the order of 10^5 and the tunable band gap of 2.1 eV [48,49]. It is observed that the lateral devices based on 2D materials consumes more energy than the vertical devices [50]. Recently, a low-power non-volatile memory switching is reported in layered 2D WS_2 device [51]. The programming voltages for both the devices are 0.35 V and 0.55 V for WS_2 and MoS_2, respectively, demonstrating the high energy efficiency devices. These findings could be useful for brain inspired computing applications [51]. WS_2:PMMA nanosheets (NSs) based memristor devices also exhibits a flexible and stable bipolar resistive switching characteristic [52]. These NSs may be helpful in building the high-performance and flexible resistive random-access memory (RRAM) devices. The devices based on WS_2:PMMA have high performance in the bent state, which enable these devices to be used in the next generation wearable device applications. The WS_2:PMMA device and its I-V characteristics are shown in Fig. 1. It is observed that the current of the low resistive state (LRS) for the device with low bending (10 nm) is around 1.4 times smaller than the device with high bending (20 nm). The on/off ratio of low bent device is of the order of 10^3 at 0.5 V. The oxide based memristors based on oxygen vacancy requires large operating current. Hence, consumes large amount of power, so it is very difficult to meet the low power consumption requirement

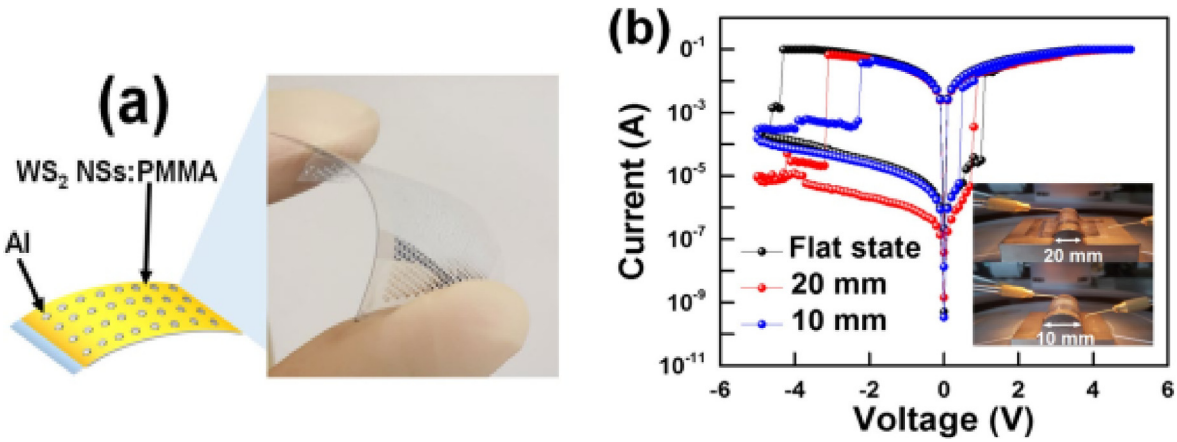

Fig. 1. (a) Schematic illustration of the device structure (b) I-V characteristics of flat and bent device. [Adapted from ref. 52]

in the oxide based memristors with oxygen vacancy. The resistive switching behavior of WS_2 based memristors depends on the W and S vacancies. It also depends on the electron hopping between different vacancies. In WS_2 based memristor devices, the defect states induced by W/S vacancies prevent the leakage current through the device thereby provide a way to realize the low power consumption memristor device for neuromorphic computing applications [53]. A schematic device of Pd/WS_2/Pt device, its I-V curve and behavior as a biological synapse is shown in Fig. 2. It is clear from Fig. 2 (b) that the device requires a large voltage sweep around 0–4 V to switch from high resistance state (HRS or OFF state) to low resistance state (LRS or ON state). The device is said to be in ON switching state or positive-SET, where the voltage at current mutations (VSET) is ≈0.6 V and the program current in the ON state is low at 1 μA. Now, switching the polarity of the device brings the device back to its initial state (HRS state). This state of the device is defined as the negative-RESET. The device has very fast SET and RESET timing approximately 13 ns and 14 ns, respectively, Fig. 2(c) and (d). The energy consumption is very close to the energy consumed by the biological synapses [54]. The current in the device depend on the pulse number, pulse interval and pulse width. Under these modulation conditions, the current of the device is very less (approximately 2 μA). It shows that the device has fast switching speed and consumes low power.

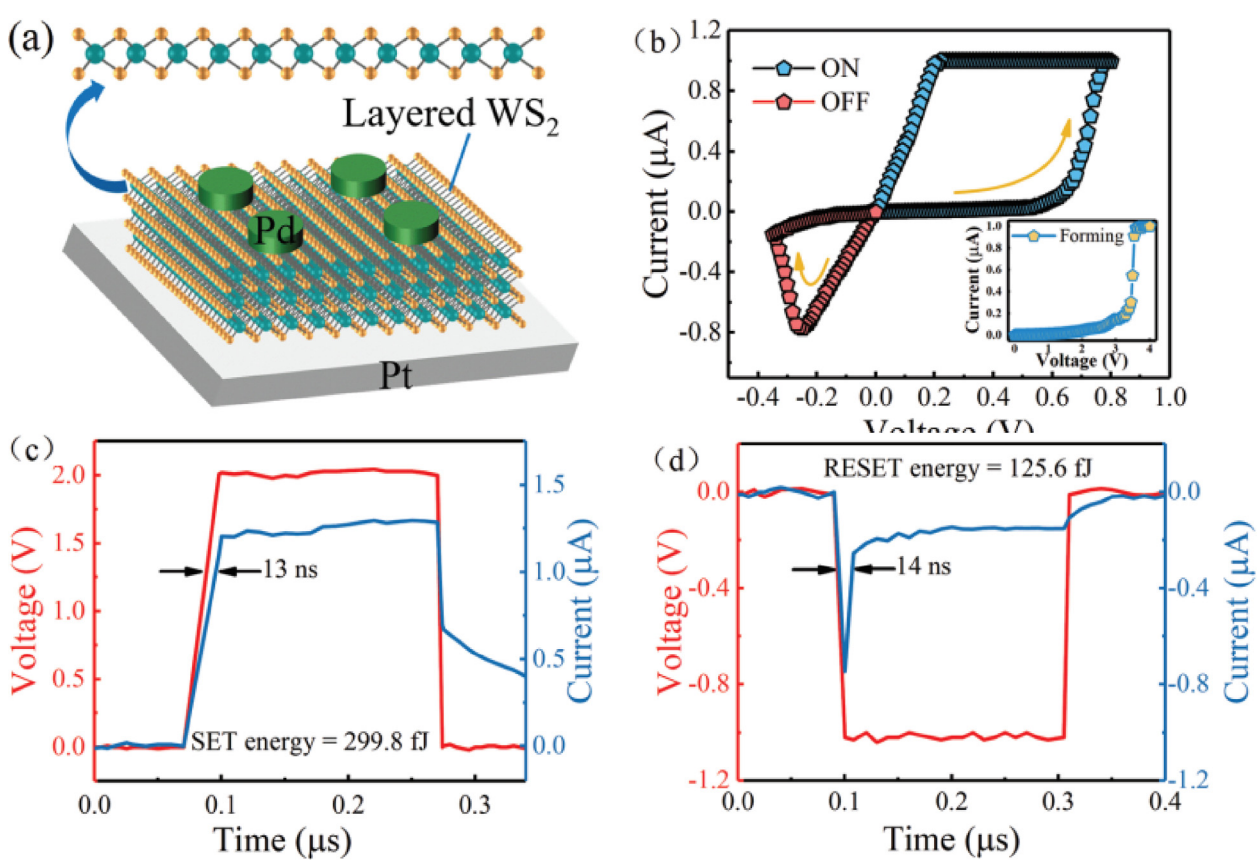

Fig. 2. (a) Schematic of Pd/WS2/Pt device. (b) The I-V characteristics of Pd/WS2/Pt device. (c) and (d) show the ON and OFF switching of the device using 13 ns and 14 ns voltage pulses, respectively. The SET and RESET energies are 299.8fJ and 125.6fJ, respectively. [Adapted from ref. 54]

Hence, it may be useful for brain inspired computing applications. Moreover, it is also seen in the biological synapse that the excessive stimulation with high frequency pulses leads to an inflection from potentiation to depression. A schematic of a biological synapse is shown in Fig. 3. Fig. 3(b) shows the paired-pulse facilitation (PPF) behavior. The postsynaptic response of the second pulse is higher than the first pulse upon receiving two successive pulses by a neuron. This phenomenon is known as PPF. The phenomenon of PPF in biological synapse is because of the increased concentration of present ionic species, which enhances the number of neurotransmitters [42]. When a memristor receives two consecutive pulse spikes, the second pulse spike generates large excitatory postsynaptic current (EPSC) compared to the first pulse spike. The amplitude of generated EPSC depend strongly on the pulse interval. It is found that this pulse time interval and EPSC amplitude is inversely proportional to each other. This behavior is shown in Fig. 3(b). Fig. 3(c) schematically illustrates the pulses applied to the device to demonstrate the spike timing-dependent plasticity (STDP). Fig. 3(d) depicts the wight change in the conductance of the memristor device. The conductance weight of the memristor increases for the pre-post condition (i.e. for $\Delta t > 0$), while it decreases for the post -pre condition (i.e. for $\Delta t < 0$). The conductance weight changes are small for large Δt. Therefore, one can conclude that the device exhibits the biological synaptic function, switching behavior based on the W/S based vacancies. The study also shows that the defects formed by the W/S vacancies localized in deep level are useful to reduce the leakage current. Hence, the device consumes low power. These characteristics of a memristor could be used to realize the future brain-inspired computing.

A resistive random-access memory (RRAM) is also a nanoscale memristor device. The reliability of this memristor device is not sufficient because of the randomness in the conducting filament. However, it can be improved with the device structure of the type $Ag/ZrO_2/WS_2/Pt$. In this device model a layer of 2D WS_2 is inserted into the memristor device to form a 2D material and oxide double-layer memristor device (2DOMD). This device exhibits high stable memristive switching and concentrated ON/OFF voltage distribution. This device has high speed, longer retention time and endurance. The 2D material and oxide-double layer memristor device has two different layers with different ion transport rates of Ag ion in the 2D material layer and oxide layer. It limits the rapture of conducting filament at the junction of two layers thereby reducing the randomness of conducting filament in memristor device because of the growth area of memristor device is shortened. Thus, the incorporation of 2D materials and oxides into a double layer memristor device can significantly enhance the practical applications of RRAM. Therefore, it may be useful in brain-enhanced computing systems for artificial synapses [55]. The enhanced reliability is not only crucial for quick and accurate information processing, however, the trivial sensitivity as well as temporal/spatial reproducibility are also equally crucial for quick and accurate information processing. All these properties are very difficult to achieve with the conventional memristors. These difficulties can be

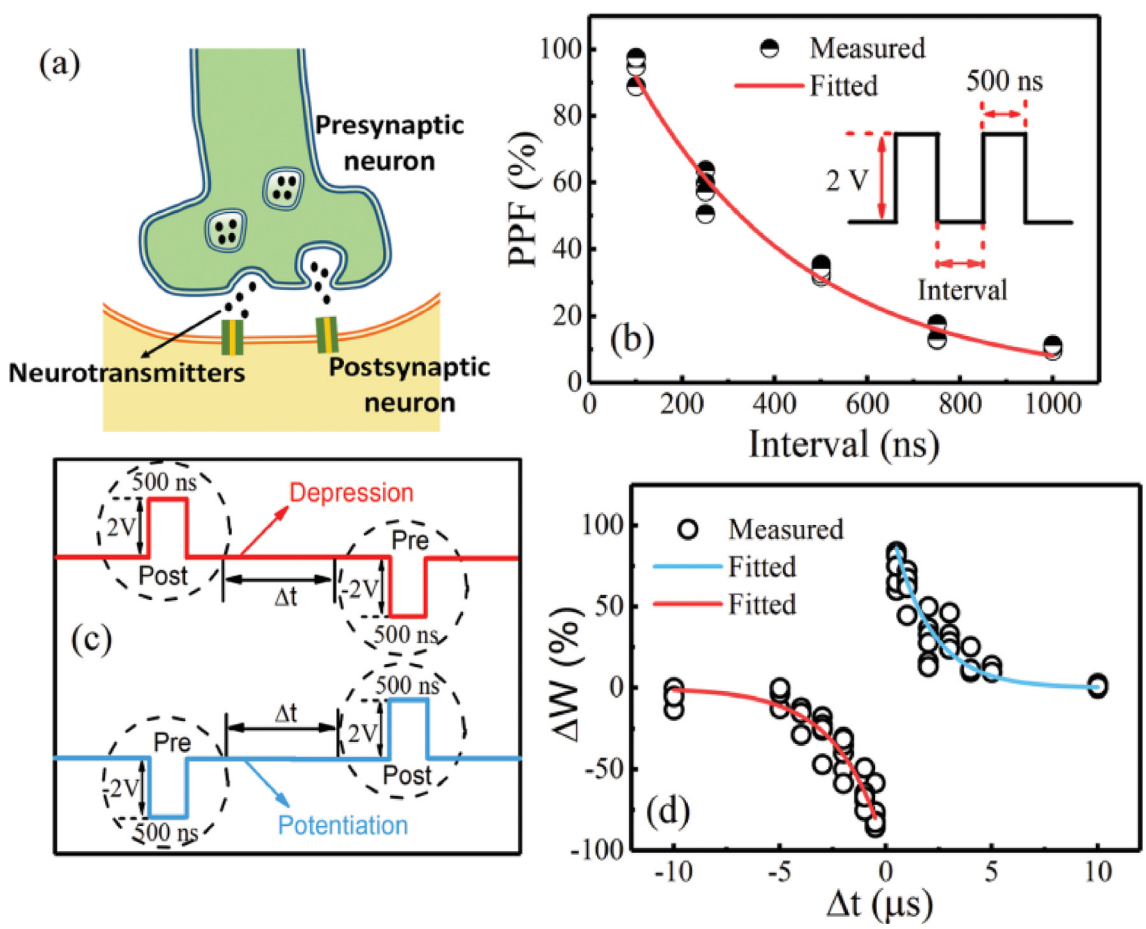

Fig. 3. (a) Schematic illustration of biological synaptic junction between presynaptic and postsynaptic neurons. (b) The paired-pulse facilitation (PPF) ratio as a function of pulse interval. The inset shows the schematic of the PPF test pulse for pulse width of 500 ns and pulse amplitude of 2 V. (c) Schematic representation of pulses applied to the device in the demonstration for spike timing-dependent plasticity (STDP). (d) Weightage change of the device with the time difference between pre- and post-neurons (Δt). It shows the STDP response. [Adapted from ref. 53]

avoided by serially connected memristors comprised of ZnO and vertically grown WS_2 layers [56]. The interlayer separation between two layers (WS_2 and ZnO) provides an effective porous medium for the growth of defective ZnO. These combination of memristor have high reproducibility of artificial synapse and robust performance. The device composed of two serially connected memrisotrs has short to long-term plasticity, spike-dependent plasticity, time dependent plasticity and paired pulse facilitation along with remarkable tunable dynamic range including comprehensive biological synaptic functions. The vertically aligned WS_2 layer significantly enhances the performance of the device due to the conduction confinement in one direction along the channel. Therefore, this robust two-terminal memristor device shows a way to fabricate a highly stable large-area neuromorphic computing device.

4. Summary and future perspectives

The present study gives a brief overview of the WS_2 based memristive devices for neuromorphic brain-inspired computing applications. The working and operation along with synaptic behavior of these devices are extensively discussed. These 2D materials-based devices have many different advantages compared with the devices based on the conventional materials. Nevertheless, these devices possess different challenges to implement 2D materials in biological synaptic devices for real-life applications. It requires large-area defect free preparation and manufacturing of materials along with high energy efficient and high integration density devices. The major challenge is to grow thickness controlled high quality large-scale 2D TMDC materials-based film. Although, there are techniques to grow TMDCs based compound 2D materials, but the industrial-scalability and controlled morphology remains challenging [57,58]. Moreover, the properties and parameters are also strongly dependent on the thickness, defect, and doping concentration. These hinder the growth of high quality and large scale 2D TMDC materials. The wafer scaled techniques are being used to transfer the high quality as prepared 2D TMDCs materials onto arbitrary substrates, which are useful for mechanically deformable 2D materials-based brain inspired computing applications. There are different techniques providing feasible wafer scaled 2D layer transfer [59,60]. The 2D TMDC materials have been more extensively explored for different applications [61–64].

CRediT authorship contribution statement

Amarjit Khuraijam: Writing – original draft. **Vipin Kumar:** Conceptualization, Visualization, Writing – review & editing. **Nilanjan Halder:** . **Anoop Kumar Mukhopadhyay:** Validation, Supervision.

Declaration of Competing Interest

The authors declare that they have no known competing financial interests or personal relationships that could have appeared to influence the work reported in this paper.

Acknowledgements

This work is financially supported under the Enhanced Seed Grant Scheme with Project Ref. No. EF/2019-20/QE04-11 provided by the Directorate of Research, Maipal University Jaipur, Jaipur 303007, Rajasthan, India.

References

[1] L. Chua, IEEE Trans. Circ. Theory 18 (1971) 507–519.
[2] Y.V. Pershin, M. Di Ventra, Adv. Phys. 60 (2011) 145–227.
[3] L.O. Chua, S.M. Kang, IEEE 64 (1976) 209–223.
[4] D.B. Strukov, G.S. Snider, D.R. Stewart, R.S. Williams, Nature 453 (2008) 80–83.
[5] R.S. Williams, IEEE 45 (2008) 28–35.
[6] F. Argall, Solid-State Electron. 11 (1968) 535–541.
[7] D. Biolek, Z. Biolek, V. Biolkova, in: European Conference on Circuit Theory and Design, 2009. ECCTD (2009), pp. 249–252.
[8] A. Rak, G. Cserey, IEEE 29 (2010) 632–636.
[9] D. Batas, H. Fiedler, IEEE 10 (2011) 250–255.
[10] T. Prodromakis, B.P. Peh, C. Papavassiliou, C. Toumazou, IEEE 58 (2011) 3099–3105.
[11] S. Kvatinsky, E. Friedman, A. Kolodny, U. Weiser, IEEE 60 (2013) 211–221.
[12] A. Chanthbouala, V. Garcia, R.O. Cherifi, K. Bouzehouane, S. Fusil, X. Moya, S. Xavier, H. Yamada, C. Deranlot, N.D. Mathur, M. Bibes, A. Barthélémy, J. Grollier, Nature Mater. 11 (2012) 860–864.
[13] D. Liu, H. Cheng, X. Zhu, G. Wang, N. Wang, Appl. Mater. Interfaces 5 (2013) 1125811264.
[14] S. Kvatinsky, M. Ramadan, E.G. Friedman, A. Kolodny, IEEE 62 (2015) 786–790.
[15] Z. Biolek, D. Biolek, V. Biolekova, Radio Eng. 18 (2009) 210–214.
[16] Y.N. Joglekar, S.J. Wolf, Eur. J. Phys. 30 (2009) 661.
[17] R.W.P.J. Kuekes, G.S. Snider, Sci. Am. Mag. 293 (2005) 72–78.
[18] D. Chabi, W. Zhao, D. Querlioz, J.O. Klein, IEEE (2011) 137–143.
[19] I. Vourkas, G.C. Sirakoulis, Microelectron. J. 45 (2014) 59–70.
[20] A. DeHon, IEEE Trans. Nanotechnol. 2 (2003) 23–32.
[21] M. Hu, H. Li, Y. Chen, Q. Wu, G. Rose, R. Linderman, IEEE Trans. Neural Netw. Learn. Syst. 25 (2014) 18641878.
[22] K. Eshraghian, K.-R. Cho, O. Kavehei, S.-K. Kang, D. Abbott, S.-M.-S. Kang, IEEE Trans. Very Large Scale Integr. (VLSI) Syst. 19 (2011) 1407–1417.
[23] Y. Ho, G. Huang, P. Li, IEEE Trans. Circ. Syst. 58 (2011) 724–736.
[24] V. Erokhin, G.D. Howard, A. Adamatzky, Int. J. Bifurc. Chaos 22 (2012) 125–283.
[25] J. Borghetti, G.S. Snider, P.J. Kuekes, J.J. Yang, D.R. Stewart, R.S. Williams, Nature 464 (2010) 873–876.
[26] A. Talukdar, A. Radwan, K. Salama, Microelectron. J. 42 (2011) 1032–1038.
[27] H. Kim, M. Sah, C. Yang, T. Roska, L. Chua, IEEE Trans. Circ. Syst. 59 (2012) 148–158.
[28] G. Howard, E. Gale, L. Bull, B. de Lacy Costello, A. Adamatzky, IEEE Trans. Evolut. Comput. 16 (2012) 711–729.
[29] Z.E. Alibart, F.D. Strukov, Nat. Commun. 4 (2013) 2072–2079.
[30] J.H. Krieger, S.M. Spitzer, in: Proceedings of the 2004 Non-Volatile Memory Technology Symposium IEEE, 2004 pp. 121–124.
[31] F. Alibart, S. Pleutin, D. Guérin, C. Novembre, S. Lenfant, K. Lmimouni, C. Gamrat, D. Vuillaume, Adv. Funct. Mater. 20 (2010) 330.
[32] F. Alibart, S. Pleutin, O. Bichler, C. Gamrat, T. Serrano-Gotarredona, B. Linares-Barranco, D. Vuillaume, Adv. Funct. Mater. 22 (2012) 609–616.
[33] O. Bichler, W. Zhao, F. Alibart, S. Pleutin, S. Lenfant, D. Vuillaume, C. Gamrat, Neural Comput. 25 (2013) 549–566.
[34] Y. Chen, G. Liu, C. Wang, W. Zhang, R.-W. Li, L. Wanga, Mater. Horiz. 1 (2014) 489–506.
[35] A.A. Bessonov, M.N. Kirikova, D.I. Petukhov, M. Allen, T. Ryhänen, M.J.A. Bailey, Nat. Mater. 14 (2015) 199–204.
[36] R. Ge, X. Wu, M. Kim, J. Shi, S. Sonde, T. Sushant, Z. Li, L. Yanfeng, C. Jack, D. Akinwande, Nano Lett. 18 (2018) 434–441.
[37] M. Kim, R. Ge, X. Wu, X. Lan, J. Tice, J. Lee, C. Jack, D. Akinwande, Nat. Commun. 9 (2018) 2524–2531.
[38] S.H. Jo, T. Chang, I. Ebong, B.B. Bhadviya, P. Mazumder, W. Lu, Nano Lett. 10 (2010) 1297–1301.
[39] D. Li, B. Wu, X. Zhu, J. Wang, B. Ryu, W.D. Lu, W. Lu, X. Liang, ACS Nano 12 (2018) 9240–9252.
[40] S.-G. Yi, M.U. Park, S.H. Kim, C.J. Lee, J. Kwon, G.-H. Lee, K.-H. Yoo, ACS Appl. Mater. Interfaces 10 (2018) 31480–31487.
[41] Z. Wang, L. Wang, M. Nagai, L. Xie, M. Yi, W. Huang, Adv. Electron. Mater. 3 (2017) 1600510–1600538.
[42] Z. Wang, S. Joshi, S.E. Savel'ev, H. Jiang, R. Midya, P. Lin, M. Hu, N. Ge, J.P. Strachan, Z. Li, Q. Wu, M. Barnell, G.-L. Li, H.L. Xin, R.S. Williams, Q. Xia, J.J. Yang, Nat. Mater. 16 (2017) 101–108.
[43] L. Zhang, T. Gong, H. Wang, Z. Guo, H. Zhang, Nanoscale 11 (2019) 12413–12435.
[44] S. Bertolazzi, P. Bondavalli, S. Roche, T. San, S.-Y. Choi, L. Colombo, F. Bonaccorso, P. Samorì, Adv. Mater. 31 (2019) 1806663–1806735.
[45] R. Ge, X. Wu, M. Kim, J. Shi, S. Sonde, L. Tao, Y. Zhang, J.C. Lee, D. Akinwande, Nano Lett. 18 (2018) 434–441.
[46] R. Lv, J.A. Robinson, R.E. Schaak, D. Sun, Y. Sun, T.E. Mallouk, M. Terrones, Acc. Chem. Res. 48 (2015) 56–64.
[47] H. Wang, C. Li, P. Fang, Z. Zhang, J.Z. Zhang, Chem. Soc. Rev. 47 (2018) 6101–6127.
[48] W. Sik Hwang, M. Remskar, R. Yan, V. Protasenko, K. Tahy, S. Doo Chae, P. Zhao, A. Konar, H. (Grace) Xing, A. Seabaugh, D. Jena, Appl. Phys. Lett. 101 (2012) 013107-4.
[49] H. Zeng, G.-B. Liu, J. Dai, Y. Yan, B. Zhu, R. He, L. Xie, S. Xu, X. Chen, W. Yao, X. Cui, Sci. Rep. 3 (2013) 1608–1615.
[50] V.K. Sangwan, D. Jariwala, I.S. Kim, K.-S. Chen, T.J. Marks, L.J. Lauhon, M.C. Hersam, Nat. Nanotechnol. 10 (2015) 403–406.

[51] C. Mihai, F. Sava, A.C. Galca, A. Velea, AIP Adv. 10 (2020) 025102–25105.
[52] J.H. Lee, C. Wu, S. Sung, H. An, T.W. Kim, Sci. Rep. 9 (2019) 19316–19318.
[53] X. Yan, Q. Zhao, A.P. Chen, J. Zhao, Z. Zhou, J. Wang, H. Wang, L. Zhang, X. Li, Z. Xiao, K. Wang, C. Qin, G. Wang, Y. Pei, H. Li, D. Ren, J. Chen, Q. Liu, Small 15 (2019) 1901423–1901429.
[54] S.B. Laughlin, R.R. van Steveninck, J.C. Anderson, Nat. Neurosci. 1 (1998) 36–41.
[55] X. Yan, C. Qin, C. Lu, J. Zhao, R. Zhao, D. Ren, Z. Zhou, H. Wang, J. Wang, L. Zhang, X. Li, Y. Pei, G. Wang, Q. Zhao, K. Wang, Z. Xiao, H. Li, ACS Appl. Mater. Interfaces 11 (2019) 48029–48038.
[56] M. Kumar, D.-K. Ban, S.M. Kim, J. Kim, C.-P. Wong, Adv. Electron. Mater. 5 (2019) 1900467–1900469.
[57] J. Chen, X. Zhao, S.J.R. Tan, H. Xu, B. Wu, B. Liu, D. Fu, W. Fu, D. Geng, Y. Liu, W. Liu, W. Tang, L. Li, W. Zhou, T.C. Sum, K.P. Loh, J. Am. Chem. Soc. 139 (2017) 1073–1076.
[58] P. Yang, X. Zou, Z. Zhang, M. Hong, J. Shi, S. Chen, J. Shu, L. Zhao, S. Jiang, X. Zhou, Y. Huan, C. Xie, P. Gao, Q. Chen, Q. Zhang, Z. Liu, Y. Zhang, Nature Commun. 9 (2018) 979–1010.
[59] J.H. Kim, T.J. Ko, E. Okogbue, S.S. Han, M.S. Shawkat, M.G. Kaium, K.H. Oh, H.S. Chung, Y. Jung, Sci. Rep. 9 (2019) 1641–1710.
[60] M. Wang, H. Li, T.-J. Ko, M.S. Shawkat, E. Okogbue, C. Yoo, S.S. Han, M.A. Islam, K.H. Oh, Y. Jung, J. Mater. Res. 35 (2020) 1350–1368.
[61] H. An, Y.H. Lee, J.H. Lee, C. Wu, B.M. Koo, T.W. Kim, Sci. Rep. 10 (2020) 5793–5798.
[62] Z. Shen, C. Zhao, Y. Qi, W. Xu, Y. Liu, I.Z. Mitrovic, L. Yang, C. Zhao, Nanomaterials 10 (2020) 1437–1531.
[63] T.-J. Ko, H. Li, S.A. Mofid, C. Yoo E. Okogbue, S.S. Han, M.S. Shawkat, A. Krishnaprasad, M.M. Islam, D. Dev, Y. Shin, K.H. Oh, G.-H. Lee, T. Roy, Y. Jung, iScience 23 (2020) 101676-31.
[64] W. Xu, J. Wang, X. Yan, Front. Nanotechnol. 3 (2021) 645995–646014.